Supplementary Material: Spatial statistics interrogate relationships between glacier thinning and fjord characteristics in Greenland

David. F. PORTER[1], K. J. TINTO[1], A. BOGHOSIAN[1], B. CSATHO[2], R. E. BELL[1], and J. R. COCHRAN[1]

SUPPLEMENTARY TABLES AND FIGURES

Figure S1. Correlogram

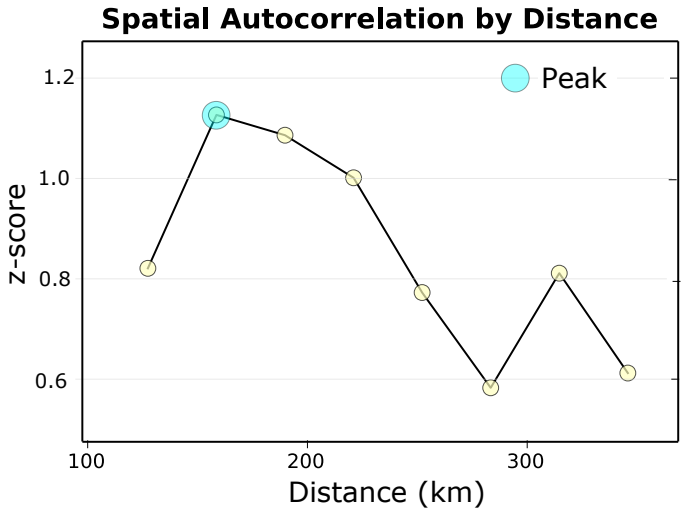

Figure S1. Spatial correlogram of dynamic thinning rates with distance between grounding lines. The peak z-score of ∼190 km is highlighted.

We construct the neighborhood weights matrix used in the spatial analysis via the inverse-distance threshold method. Appropriate for investigation of oceanic forcing of tidewater glacier termini, closer observations are weighted more strongly up until a pre-defined limit. We chose this threshold by iteratively autocorrelating glacier thinning rates at increasing distances and recording local maxima in z-scores. The z-score increases with larger distance threshold until ∼180 km (*Supp. Fig. S1*), After which there is a persistent decline in z-scores. We increase the limit to 193 km for the neighborhood weights matrix to ensure that even glaciers in the remote North have at least four neighbors in the spatial analysis. This radius is also comparable to the typical length scale of ocean eddies (Zhang et al., 2014).

Figure S2. Additional Regional Regressions

The OLS regressions of ocean heat content (OHC) with the maximum dynamic thinning rate for the remaining three regions (”Thule”, ”North”, and ”Scoresby Sund”) are presented in **Figure S2**. In the North and Thule regions, the range of dynamic thinning rates and OHC both fall within a narrower range than the

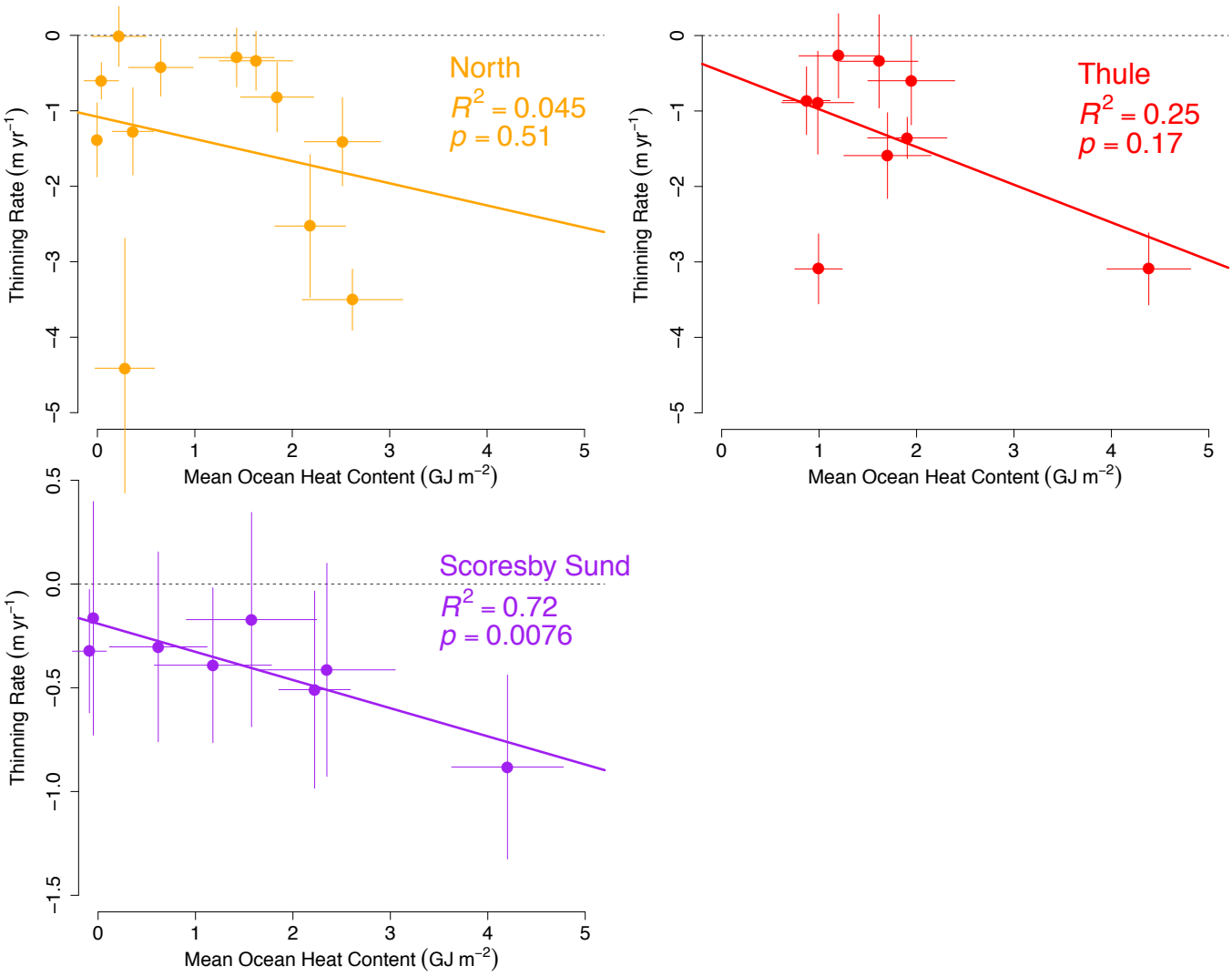

Figure S2. OLS regression of ocean heat content (OHC) in $GJ\ m^{-2}$ with the maximum dynamic thinning rate for each catchment ($m\ yr^{-1}$) for the a) North, b) Thule, and c) Scoresby Sund regions. The coefficient of determination R^2 shown for each regional subset.

full glacier set. However, most observations cluster close to the origin with just a few glaciers with higher thinning rates and OHC, resulting in an insignificant coefficient of determination.

As a whole, the Scoresby Sund region (n=8) in Northeast Greenland is one of the more stable regions in terms of dynamic thinning (**Figure S2**). Glaciers in this region have receded far into their glacier troughs, leaving behind long fjords that inhibit their connection with waters on the shelf. Consequently, dynamic thinning rates for glaciers in Scoresby Sund region are all below 1 $m\ yr^{-1}$. The glacier with the highest thinning rates here is Dendritic glacier, earlier identified as a spatial outlier. Although more stable as a whole, the OLS regression of dynamic thinning rate on OHC for this regions is significant (p =0.008) with an R^2 of 0.72. The slope of the regression line is shallower (yet still significant) than that for other regions, suggesting that the effect of a deeper grounding line is smaller in this region. This apparent reduced sensitivity could be related to these glaciers lying a long distance from the mouths of fjords.

Figure S3. Regional Regressions using Bed Machine Version 3

In addition to the gravity and radar-derived grounding line depths of the 74 Greenland tidewater glaciers in this study, we repeat the regression analysis using output from Bed Machine version 3 (Morlighem et al., 2017). Bed Machine uses the conservation of mass as the basis for a physically-based method of interpolating between ice thickness observation. Over the Greenland ice sheet, this results in a complete, data-constrained gridded ice thickness product. Grounding line depths were extracted from Bed Machine using the across-glacier velocity maximum (Rignot and Mouginot, 2012) nearest the grounding line as could be determined, contributing 126 new grounding line depths.

New OLS regression models using Bed Machine grounding line depths are similar to the regression using just the 74 glaciers from the present study (**Figure S3**). The qualitative pattern of deeper-grounded glaciers thinning at a higher rate remains, though with a slightly reduced R^2 of 0.14 ($p <<<0.001$). In general, the two sets of depths agree quite well, especially for glaciers deeply grounded glaciers. However, a majority of the additional grounding line depths introduced by using the gridded Bed Machine product are shallower than $\sim$200 m, resulting in a smaller slope of the line-of-best-fit. Consistent with our previous findings, these shallow glaciers are in general thinning less than their deeper counterpoints. Importantly, there are many glaciers in Bed Machine version 3 with grounding lines above the PW/AW boundary of $\sim$150 m, including many grounding lines at or above sea level. This is due, in part, to increasing errors in Bed Machine ice thickness estimates with distance from radar sounding constraints. Near the terminus, where radar attenuation hampers unambiguous identification of the ice-rock interface, Bed Machine errors can be large. Mean grounding line depth uncertainty for the 200 glaciers from Bed Machine **Figure S3** is $\pm$68 m, with a maximum uncertainty of 227 m for 79°N. When these shallow and uncertain glaciers are excluded, the overall relationship between grounding line depth and thinning rate is similar whether Bed Machine-interpolated or directly-radar-sensed data are considered.

The bed machine dataset increases the number of grounding line depth estimates around Greenland but with greater uncertainty than the directly-measured depths or radar-constrained gravity models. We have restricted the scope of this study to test the relationship between ocean heat content and glacier thinning rates. Many other parameters may be significant in controlling the variability of thinning rates around Greenland. Further work considering a broader range of parameters would benefit from the inclusion of bed machine interpolated grounding line depths.

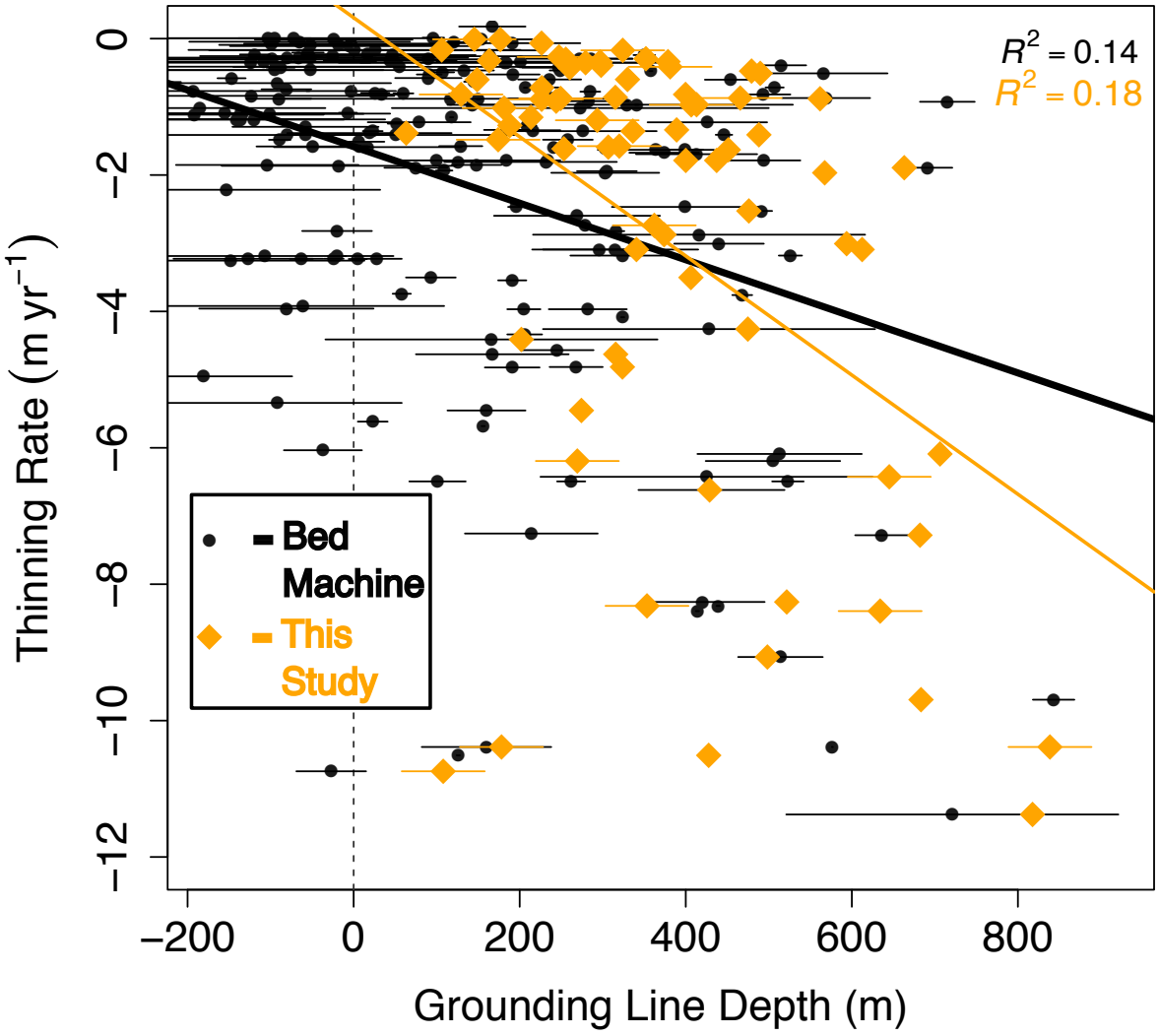

Figure S3. OLS regression of grounding line depth (m) with the maximum dynamic thinning rate for both glaciers in this study (n = 74, orange) and from Bed Machine Version 3 (n = 200, black). The coefficient of determination R^2 and best-of-fit line is shown for both sets.

Table S1.

	Name	Lat °N	Lon[a] °E	Grounding Line[b] *meters*	Sill Depth[c] *meters*	Mean OHC $GJ\ m^{-2}$	dH/dt[d] $m\ yr^{-1}$
1	Jakobshavn Isbrae	69.15	-49.60	-683.30		5.12	-9.69
2	Eqip Sermia	69.80	-50.20	-213.50		1.79	-1.15
3	Kangilerngata Sermia	69.90	-50.30	-253.20		2.29	-1.62
4	Sermeq Kujalleq	70.00	-50.20	-413.00		4.10	-0.97
5	Sermeq Avannarleq	70.05	-50.30	-226.30		1.92	-0.07
6	Store Gletscher	70.39	-50.60	-406.60		4.03	-0.97
7	Kangerlussuup Sermersua	71.47	-51.40	-226.60		1.08	-0.72
8	Rink Isbrae	71.75	-51.60	-465.60		3.26	-0.87
9	Umiammakku Isbrae	71.73	-52.40	-427.60		2.94	-10.51
10	Inngia Isbrae	72.04	-52.60	-315.60		1.91	-4.63
11	Upernavik Isstrom S	72.85	-54.40	-634.10	-430	5.35	-8.39

12	Upernavik Isstrom C	72.94	-54.30	-498.30	-490	4.02	-9.07
13	Unnamed near Upernavik	73.02	-54.30	-838.60	-695	7.02	-10.39
14	Qeqertarsuup Sermia	73.59	-55.60	-389.00	-525	2.80	-1.34
15	Illullip Sermia	74.41	-56.00	-593.70	-406	4.74	-3.01
16	Alison Gletscher	74.62	-56.00	-270		1.71	-6.19
17	Unnamed south Hayes M	74.79	-56.60	-428.70	-374	3.26	-6.62
18	Steenstrup Gletscher	75.28	-58.00	-274.30	-205	1.49	-5.45
19	Sverdrup Gletscher	75.58	-58.10	-521.60	-408	3.38	-8.26
20	Nansen Gletscher	75.73	-58.90	-451.30	-360	3.12	-1.63
21	Kong Oscar Gletscher	75.99	-59.80	-663.10	-369	4.93	-1.89
22	Unnamed north Oscar	76.07	-59.90	-437.20	-191	3.00	-1.79
23	Issuuarsuit Sermia	76.06	-60.60	-400.00	-240	2.65	-1.79
24	Rink Gletscher	76.24	-60.90	-249.30	-176	1.26	-0.88
25	Carlos Gletscher	76.42	-63.40	-329.80	-292	1.95	-0.60
26	Yngvar Nielsen Brae	76.38	-64.10	-296.90	-179	1.61	-0.34
27	Savissuaq Gletscher	76.33	-65.50	-247.40	-176	1.20	-0.27
28	Nigerlikasik	76.24	-67.30	-226.40		0.99	-0.89
29	Alangorliup Sermia	76.60	-67.80	-306.70		1.70	-1.59
30	Heilprin Gletscher	77.53	-66.00	-336.30		1.90	-1.36
31	Tracy Gletscher	77.66	-66.10	-612.40		4.38	-3.09
32	Humboldt Gletscher	79.80	-64.70	-188.10		0.36	-1.27
33	Newman Bugt	81.33	-57.30	-176.70		0.22	-0.01
34	Steensby Gletscher	81.47	-54.40	-378.60		1.63	-0.34
35	Ryder Gletscher	81.57	-50.40	-399.70		1.84	-0.82
36	C.H.Ostenfeld gletscher	81.60	-45.30	-352.00		1.43	-0.29
37	Marie Sophie gletscher	81.79	-32.80	-148.70		0.04	-0.60
38	Academy Gletscher	81.64	-32.50	-260.30		0.65	-0.43
39	Hagen Brae	81.44	-27.40	-202.00		0.28	-4.41
40	Zachariae Isstrom	78.78	-21.20	-406.20		2.62	-3.50
41	Marie Gletscher	77.52	-21.60	-63.30		-0.00	-1.39
42	Gerard de Geer Gl. N	73.50	-27.30	-163.30		-0.09	-0.32
43	Gerard de Geer Gl. S	73.46	-27.40	-255.50		0.62	-0.30
44	Morell Gletscher	73.13	-27.70	-381.20		2.35	-0.41
45	F. Graae Gletscher	72.11	-28.70	-298.00		1.18	-0.39
46	Daugaard-Jensen	71.91	-28.60	-489.70		2.22	-0.51
47	Vestfjord Gletscher	70.39	-29.10	-561.70		4.20	-0.88
48	Sydbrae	70.20	-26.30	-106.10		-0.05	-0.17
49	Bredegletscher	70.27	-25.20	-324.10		1.58	-0.17
50	Dendritgletscher	69.29	-25.20	-129.40		-0.10	-0.82
51	Kangerlussuaq Gletscher	68.60	-32.90	-817.60		27.38	-11.38
52	Polaric Gletscher	67.87	-32.50	-243.90		0.73	-0.92
53	K.I.V. Steenstrup Nodre	66.50	-34.50	-279.30		1.47	-0.35
54	Midgardgletscher	66.47	-36.70	-107.90		0.11	-10.74
55	Fenrisgletscher	66.36	-37.50	-474.80		13.07	-4.26
56	Helheimgletscher	66.37	-38.20	-682.10		18.51	-7.28

57	Koge Bugt C	65.17	-41.10	-567.30		8.00	-1.97
58	Koge Bugt S	64.98	-41.20	-323.70		3.67	-4.81
59	Umiivik Fjord	64.48	-40.70	-181.20		1.34	-1.02
60	Graulv	64.33	-41.50	-373.90		4.56	-2.87
61	A.P. Bernstorff Gl.	63.84	-41.70	-645.10		13.91	-6.43
62	Skinfaxe	63.21	-41.80	-145.40		0.79	-0.01
63	Rimfaxe	63.21	-42.20	-479.20		8.05	-0.48
64	Heimdal Gletscher	62.86	-42.60	-362.10		3.95	-2.74
65	Tingmiarmiut Fjord	62.76	-43.20	-706.20		12.99	-6.09
66	Kangiata Nunaata Sermia	64.30	-49.60	-174.10		1.58	-1.48
67	Narsap Sermia	64.64	-50.00	-319.90		6.87	-1.58
68	Petermann Gletscher	80.55	-59.70	-476.00		2.18	-2.53
69	Docker Smith Gl. W	76.31	-62.00	-353.30	-291	2.10	-8.32
70	Unnamed near Upernavik	73.03	-54.50	-178.10	-600	0.98	-10.39
71	Farquhar Gletscher	77.70	-66.20	-340.60		0.99	-3.09
72	Melville Gletscher	77.73	-66.60	-315.20		0.87	-0.86
73	Nioghalvfjerdsfjorden (79°C)	79.25	-22.40	-488.10		2.52	-1.41
74	Puisortoq S	61.92	-42.60	-293.40		2.95	-1.20

[a]Mean location of grounding line depth estimates.

[b]Average of Gravity-modeled and radar-determined water depths.

[c]Minimum water depth from OIB gravity and OMG echosounder data.

[d]Catchment-maximum dynamic thinning rate.

REFERENCES

Morlighem, M., Williams, C. N., Rignot, E., An, L., Arndt, J. E., Bamber, J. L., et al. (2017). BedMachine v3: Complete Bed Topography and Ocean Bathymetry Mapping of Greenland From Multibeam Echo Sounding Combined With Mass Conservation. *Geophysical Research Letters* 44, 11,051–11,061

Rignot, E. and Mouginot, J. (2012). Ice flow in Greenland for the International Polar Year 2008–2009. *Geophysical Research Letters* 39, L11501–

Zhang, Z., Wang, W., and Qiu, B. (2014). Oceanic mass transport by mesoscale eddies. *Science* 345, 322–324